Fluvial tufa evidence of Late Pleistocene wet intervals from Santa Barbara, California, U.S.A

Yadira Ibarra[1*]; Frank A. Corsetti[1]; Sarah J. Feakins[1]; Edward J. Rhodes[2]; Matthew E. Kirby[3]

[1] *University of Southern California, Department of Earth Sciences, 3651 Trousdale Avenue, Los Angeles, CA 90089, USA*

[2] *University of California, Los Angeles, Department of Earth and Space Sciences, 595 Charles Young Drive East, Los Angeles, CA 90095, USA*

[3] *California State University Fullerton, Department of Geological Sciences, Fullerton, CA 92834, USA*

[*] Corresponding author: yibarra@usc.edu

Abstract

Past pluvials in the western United States provide valuable context for understanding regional hydroclimate variability. Here we report evidence of conditions substantially wetter than today from fluvial tufa deposits located near Zaca Lake, Santa Barbara County, California that have been dated by radiocarbon (^{14}C) and Infra-Red Stimulated Luminescence (IRSL). Two successions of tufa deposition occur within a small catchment that drains Miocene Monterey Formation bedrock: 1) a fluvial deposit (0−0.5 m thick, 200 m in extent) that formed along a narrow valley below a modern spring, and 2) a perched deposit about 10 m higher (2 m thick, 15 m in extent). IRSL and radiocarbon dating of the perched carbonates suggests at least two episodes of carbonate growth: one at 19.4 ± 2.4 (1σ) through 17.8 ± 2.8 (1σ) ka and another at 11.9 ± 1.5 (1σ) ka verified with a charcoal ^{14}C age of 10.95 ± 0.12 (2σ) cal ka BP. The relationship between the perched and fluvial spring deposits is inferred to represent a drop in the water table of more than 10 m associated with a transition from a wet climate in the late glacial to a dry Holocene today.

The wet period indicated by tufa growth between 19.4 and 17.8 ka is relatively consistent with other California climate records both north and south of Zaca Lake. However, tufa growth ca. 12 to 11 ka demonstrates wet conditions occurred as far south as Zaca Lake during the Younger Dryas event, in contrast to climate records farther south in Lake Elsinore indicating persistently dry conditions through this interval. A small shift north in the average position of the winter season storm track could explain wet winters at Zaca while at the same time generating dry winters at Lake Elsinore, 275 km southwest of Zaca. If true, these data indicate that rather small latitudinal shifts in the average winter season storm track can produce large changes in regional hydroclimate.

Keywords: tufa; pluvial; palaeoclimate; Infra-Red Stimulated Luminescence; radiocarbon

1. Introduction

With concern over the projected aridification of the southwestern US (Seager et al., 2007, Williams et al., 2012), there is heightened interest in characterizing past evidence for extended pluvial periods and droughts in California's pre-instrumental record to better understand the large scale controls on climate and how these may change in the future. The western United States (western US) experienced a wetter climate during the Last Glacial Maximum (18-20 ka cf. Denton et al., 2010) relative to present as evidenced by palaeolakes Bonneville and Lahontan (Benson, 1990), as well as expanded palaeolakes Estancia and Mojave (Allen and Anderson, 2000; Anderson et al., 2002; Wells et al., 2003). Additional evidence for wetter conditions comes from elevated and expanded palaeolake shorelines in Owens Valley (Mensing, 2001), higher sand contribution to profundal sediments in Lake Elsinore (Kirby et al., 2013), isotopic evidence from speleothems in New Mexico and Arizona (Asmerom et al., 2010; Wagner et al., 2010), and evidence for vegetation change based on (1) plant leaf waxes from Lake Elsinore sediments (Kirby et al., 2013) and (2) pollen from marine sediments in the Santa Barbara Basin (Heusser and Sirocko, 1997). Detailed analyses of those proxy records with high temporal resolution and improved dating precision have revealed that temperature and hydroclimate were spatially and temporally variable across the western US in the late glacial and across the deglacial (Lyle et al., 2012; Kirby et al., 2013). In particular, pollen records from marine sediments offshore southern and northern California and Oregon reveal variable timing of hydroclimatic change along the coast (Lyle et al., 2010; 2012). Adding records that concentrate on the spatial and temporal picture are key to resolve the history and causes of hydroclimatic variability for specific regions across the western US (e.g., coastal versus inland). Presently there are few terrestrial records from coastal southern California that address hydrological balance at the LGM and across the last deglacial (e.g., Heusser and Sirocko, 1997; Kirby et al., 2013).

1.1 Tufa evidence for pluvials

Spring-associated carbonates generated from carbonate-rich, ambient temperature groundwater, referred to hereafter as 'tufa' *sensu* Pedley (1990), serve as potential archives of source waters and climate of their local region (Andrews, 2006). Notably, the presence of large tufa accumulations in arid and semi-arid regions is indicative of periods of accelerated groundwater recharge, as carbonate will only form when there is a net recharge to the groundwater aquifer (Pedley, 1990). Tufa deposits are therefore robust indicators of past pluvials (Szabo, 1990; Crombie et al., 1997; Auler and Smart, 2001; Viles et al., 2007), and may serve as proxy records of hydrological balance to complement other local proxy records of palaeoclimate (e.g., Garnett et al., 2004; Dominguez-Villar et al., 2007; Cremaschi et al., 2010).

The western US hosts several tufa deposits, including the well-known towers and pinnacles from lakes in Nevada and California (Scholl, 1960; Newton and Grossman, 1988; Benson, 1994; Li et al., 2008). Climate reconstructions from these lacustrine tufa deposits and related lake sediments have added support to the idea the Last Glacial Maximum (LGM) in the Great Basin was wetter than today (e.g., Benson, 1978). However, records of *fluvial* tufa deposits are less well-known (e.g., Barnes, 1965) as they are perhaps less conspicuous compared to their *lacustrine* counterparts in the present semi-arid climate of southern California.

Here we present compelling terrestrial evidence of persistent wet conditions based on fossil and recent fluvial tufa deposits from a coastal site near Zaca Lake, in Santa Barbara County, California (Fig. 1). Radiocarbon and IRSL dating allow us to constrain the age of these deposits. We combine geomorphic, textural, petrographic, and geochemical observations to evaluate the nature of the depositional environment during this wet interval. We compare these new findings to other terrestrial and marine records towards better understanding of the regional patterns and the magnitude, timing, and causes of pluvial conditions in coastal southern California.

2. Geologic and environmental setting

Two successions of spring-associated carbonate deposits have been described from the Zaca Lake catchment ~3 km east of Zaca Lake in Santa Barbara county, California (Fig. 2; Ibarra et al., 2014). One succession occurs along a narrow valley (referred to hereafter as 'fluvial' carbonates) and extends discontinuously for about 200 m with an overall drop in elevation of about 40 m. The other succession occurs perched upon the slope of the north ridge (referred to here as 'perched' carbonates) about 10 m above the fluvial carbonates (Fig. 2). The carbonates formed within a relatively small catchment, and drape over Miocene Monterey Formation bedrock (Fig. 1A). About 100 years ago, the spring was boxed and piped for human consumption (Norris and Norris, 1994) which continues to the present day, such that carbonate deposition downstream is likely not active along the entirety of the fluvial path (Ibarra et al., 2014). The residence time of water in the catchment is relatively short as fluctuations in the water table on the order of years to decades have been observed in historical documents (Norris and Norris, 1994), and they are associated with known fluctuations in recorded precipitation for the region (SBB Water Works, 2013). The sensitivity of the spring to decadal scale climatic fluctuations suggest that the carbonate precipitation associated with the spring may record decadal or longer variations in precipitation.

Santa Barbara County is characterized by a Mediterranean climate (warm, dry summers and cool, wet winters). The region receives about 700 mm of rain each year, with >80% of the precipitation delivered during the winter between October and March (Cayan and Roads, 1984). Moisture is advected by westerly winds from the Pacific Ocean (Fig. 1). Knowledge of inter-annual precipitation variability is limited by the short instrumental record: rain gauge measurements in Santa Barbara extend back to the 1860s (SBB Water Works, 2013). Proxy evidence can extend our perspective of hydroclimate in the region and is the only way to capture evidence for multi-decadal to millennial scale droughts and pluvials in the west (Briggs et al., 2005; Cook et al., 2004; Mensing et al., 2013). The sediments of Zaca Lake have yielded records of hydroclimate fluctuations over the last 3,000 years including pluvials lasting decades to centuries based on leaf wax, pollen, and grain size evidence (Feakins et al., 2014; Dingemans *in review*, Kirby et al, *in review*). Tufa deposits within the catchment provide evidence for pluvial conditions back to ca. 20 kyrs as outlined below.

3. Spring carbonate facies

3.1.1 Fluvial carbonates

Carbonates from the fluvial deposits extend for about 200 m from the location of the spring box to the bottom of the fluvial cascade. However, their distribution is patchy and they exhibit a maximum thickness of about 0.5 to 1 m. The change in elevation from the spring box to the top of the fluvial cascade is about 40 m. The most prominent facies are barrage, narrow channels, and a terminal fluvial cascade unit (Fig. 2). The terminal cascade facies is about 0.5 m thick and exhibits a drop in elevation from the top to the bottom of the cascade of about 10 m (Fig. 3A). Two distinct carbonate textures drape the surface of the cascade unit (Fig. 3B): (1) a basal white unit heavily encrusted in detrital molds and organic plant debris (Figs. 3B-D) and (2) a darker, brown surficial carbonate fabric that drapes the underlying white layer and forms small (~20 cm) dams across the cascade deposit (Fig. 3B). Carbonates along the fluvial unit are distinctly banded (Fig. 3E). The bands are microscopically composed of alternating isopachous sparry and micritic laminae (Fig. 3F). Some bands contain ubiquitous calcite microphyte molds, including the calcite microstructure of the desmid microalgae *Oocardium stratum* consistent with depositional water temperatures of ~11 to 16 °C and corroborated by $\delta^{18}O$ palaeothermometry (Ibarra et al., 2014).

3.1.2 Perched carbonates

About ten meters above the present-day spring orifice, perched carbonate cascade deposits occur at the break of the valley-side slope on the north ridge (Fig. 2), representing a perched spring line tufa facies (Pedley, 1990). Perched spring line tufa is largely controlled by the slope and rate of water flow over the deposit. Perched springs give rise to prograding carbonate cascade facies, most of which built outwards resulting in vertical and lateral growth to form a prominent apron (see Pedley, 1990). Carbonate will prograde in the direction of water flow and continue to accumulate until the piece fractures (e.g., Pentecost and Zhang, 2008). Similarly, at our site, a large ~1 m-thick and ~4 m long detached block is oriented so that the cascading face rests against the wall and the opposite end plunges towards the valley channel forming a blind cave with the cascade wall (Fig. 4A). Adjacent to the large dipping piece, the cascade wall exhibits distinct carbonate curtains (*sensu* Pedley 1990; Figs. 4B-C). Downslope from the perched cascade, large talus blocks (up to ~2 m in diameter) lie unconformably along the side slope and the bottom of the valley channel (Fig. 4D). Carbonate samples from the perched cascade are highly indurated. The carbonate texture is typified by mesoscopic (~0.5 to 1 cm diameter) vuggy pore space (Fig. 4F). Microscopically, the fabric is dominantly composed of microspar, micrite, and dog-toothed spar with an irregular, heterogeneous distribution (Fig. 4G).

4. Methods

4.1. Sample collection

Samples from the fluvial carbonates were collected from the top ~20 cm of areas along the flow path that contain prominent carbonate accumulation (areas labeled in Fig. 2). Carbonate from the perched cascade deposit was not easily removed due to the massive and indurated nature of the deposit. We utilized a handheld drill with a 3 cm diameter drill bit to collect two cores. One core (70 cm long) was collected from the perched cascade face drilled horizontally into the cascade wall. A second ‘dark’ core (63 cm long) was collected behind the large detached carbonate block and immediately transferred into light-proof bags for subsequent IRSL (Fig. 5A).

4.2 Age control

4.2.1 Radiocarbon

Ten Accelerator Mass Spectrometry (AMS) ^{14}C dates were obtained from carbonate and organic fragments collected from both of the carbonate deposits. Three pieces of plant debris were hand picked from within carbonate pieces from the fluvial cascade (~20 cm depth) for subsequent $\Delta^{14}C$ analyses. We also dated two organic pieces (detrital twig and root) collected near the barrage facies (Fig. 2) that each contained concentrically encrusted carbonate (see Fig. 5B); the associated encrusted carbonate was also analyzed for $\Delta^{14}C$. Carbonate pieces of distinct growth phases from the fluvial cascade were also collected for $\Delta^{14}C$ analyses (see numbered labels in Fig. 3B). We also collected carbonate samples from a large block adjacent to the detached perched cascade. One of these samples was composed of carbonate-cemented clasts of shale from the Monterey Formation and included a charcoal clast suitable for $\Delta^{14}C$ analysis. Samples were sent to the UC Irvine Keck Laboratory for radiocarbon analysis. $\Delta^{14}C$ values were converted to calendar years before present using the CALIB 7.0.1 Program (Stuiver et al., 1998), and the CALIBomb Program (Reimer et al., 2013).

4.2.2 Infra-Red Stimulated Luminescence (IRSL)

A ~63 cm long, 4 cm diameter 'dark' core was drilled from a large (~1.5 m thick, ~3 m long) detached piece of the perched cascade unit (Fig. 5A) for luminescence dating. The core was extracted and immediately transferred into light-proof black bags for transport to the laboratory.

The carbonate core was split into five sections under controlled amber and red laboratory lighting. Two 10 cm core lengths were cut at each end of the core for dose rate estimation, and the remaining material cut into three sections of approximately 14 cm in length. The three core sections for dating were each subsequently placed in 3% HCl to dissolve carbonate, ventilated, but shielded from all light. Acid was replaced until each section of core had dissolved (up to two weeks), and no further reaction occurred when fresh acid was added. The residual material was then treated as a standard sediment sample, incorporating the following steps. The samples were first wet sieved to isolate the 175 – 200 μm fraction. Potassium feldspars were floated from these fractions using a lithium metatungstate solution of density 2.58 g cm^{-3}. After rinsing and drying, these samples provided just a few hundred grains.

Luminescence dating was performed using a single grain post-IR IRSL approach, based on the single aliquot regenerative-dose (SAR) method of Baylaert et al. (2009). Measurements were performed using a Risø automated TL-DA-20D reader fitted with a dual laser single grain attachment. Stimulation was provided by a 150 mW 830 nm IR laser at 90%, and luminescence signals were detected using an EMI 9235QB photomultiplier tube, fitted with a BG3 and BG39 filter combination, allowing transmission in the blue (340 - 470 nm). To reduce thermal transfer and contributions from slowly bleaching signals, samples were bleached at raised temperature using Vishay TSFF 5210 870 nm IR diodes.

The SAR protocol used involves repeated cycles with the following steps: 1) Regenerative beta dose (0 for the natural cycle), 2) Preheat, 60 s at 250 ºC, 3) IRSL$_{50}$, 2.5 s per grain at 50 ºC, 4) IRSL$_{225}$, 2.5 s per grain at 225 ºC, 5) Test dose, 9.5 Gy, 6) Preheat, 60 s at 250 ºC, 7) IRSL$_{50}$, 2.5 s per grain at 50 ºC, 8) IRSL$_{225}$, 2.5 s per grain at 225 ºC, 9) Hot bleach, 40 s IRSL using diodes at 290 ºC. The measurement sequence included SAR cycles comprising the natural measurement, four regenerative-dose points, a zero dose point to assess thermal transfer, and a repeat of the first dose point to assess recycling. This approach has provided a number of age estimates spanning 400−80,000 years consistent with independent age control provided by ^{14}C and ^{10}Be (Rhodes, submitted).

Most grains measured provided no significant IRSL signal, but a proportion of grains displayed strong IRSL decays, with linear or saturating growth with increasing regenerative dose. A degree of variation between the equivalent dose estimates of different grains in each sample was observed, interpreted as incomplete zeroing of some grains incorporated as the tufa was building. For each of the three samples, the minimum group of grains, defined as those consistent with an overdispersion of 15%, was selected; grains with higher dose values were rejected from the analysis.

Dose rate estimation was conducted using ICP-OES for K content, and ICP-MS for U and Th, using the conversion factors of Adamiec and Aitken (1998). The resulting age estimates are provided in Table 2. We expect that most of the dose rate contributions are from sediment grains contained within the tufa, but we recognize that tufa can absorb U from water, and the possibility exists of U disequilibrium. In this case, the ICP-MS estimate of ^{238}U will overestimate the dose rate; the U lacks daughter isotopes lower in the decay series, and this effect can roughly half the beta dose rate from U and have an even more dramatic effect on the U gamma dose rate (as most gamma energy is provided by isotopes at the end of the U decay series). To assess the potential magnitude of this effect, we have also calculated the age estimates with 50% of the U beta dose rate, and no U gamma contribution. We note that this represents an extreme condition – in practice some or most of the U dose rate contributions probably come from sediment grains, and for these contributions, we expect secular equilibrium to exist. The age estimates assuming extreme U disequilibrium (as described above) range from 1 to 2 ka older than those presented in Table 2. We consider, therefore, that this effect is likely not disrupting these age estimates significantly. We note the relatively large measurement uncertainties, caused by having relatively few sensitive grains contributing, and present the age estimates without allowing for potential disequilibrium effects.

4.3. Carbonate isotopic analyses

Isotopic analyses of carbonate oxygen and carbon were conducted on an Elementar Americas Inc. (Micromass Ltd) Isoprime stable isotope ratio mass spectrometer (IRMS) with a multi-prep/carbonate device and dual inlet in the Stott lab at the University of Southern California. Samples were measured relative to CO_2 reference gas calibrated against the NBS-19 ($\delta^{18}O$ value +2.20‰, $\delta^{13}C$ value +1.95‰) carbonate standard, which allows for normalization to the 2-point VPDB-LVSEC isotopic scale. The precision of this determination is better than 0.06‰ and 0.04‰ (1σ, n = 20) for $\delta^{18}O$ and $\delta^{13}C$, respectively. A working standard (carbonate,

$\delta^{18}O$ −1.88‰, $\delta^{13}C$ value of +2.07‰) monitors precision during the course of the run to 0.07‰ and 0.04‰ (1σ, n = 14) for $\delta^{18}O$ and $\delta^{13}C$, respectively.

5. Results

5.1 Age Control

5.1.1 Radiocarbon

Radiocarbon results are listed in Table 2. The piece of charcoal extracted from the perched cascade has a calibrated age range of 10,830−11,070 cy BP (2σ). All of the organic fragments from the fluvial deposit contain excess ^{14}C indicating a significant presence of radiocarbon from nuclear weapons testing during the 1960s. Samples with excess ^{14}C have estimated age ranges from about 1987 to 2007 (Table 2). The carbonate that encrusted the organic fragments from the fluvial deposits exhibit ages of 10,272 and 18,478 cy BP (Table 2). Given that the encrusted organic matter recorded modern ages ^{14}C dating of the encrusting carbonate, which revealed much older dates, does not accurately reflect the timing of carbonate deposition, and is not used here for temporal reconstruction. The ^{14}C ages on carbonate likely reflect mixing of soil derived CO_2 with old bedrock carbon and are therefore not viewed as robust to the uncertainties of fraction of ancient carbon so are not considered meaningful although we do note they are entirely consistent with values obtained on dating the charcoal and IRSL (Table 1 and Table 2).

5.1.2 IRSL

Three IRSL measurements were obtained for the extracted core (Table 1). The ‘inner’ piece yields a date of 19.4 ± 2.4 (1σ) ka, the ‘middle’ piece an age of 17.8 ± 2.8 (1σ) ka, and the ‘outer’ piece an age of 11.9 ± 1.5 (1σ) ka. These measurements of IRSL-based age corroborate the stratigraphic order we would expect given the direction of flow and growth pattern of perched tufa (Fig. 5A) and are entirely consistent with the charcoal ^{14}C age from the same deposit.

5.2. Carbonate stable isotopes

Stable carbon and oxygen isotope values from the fluvial and perched cascade are listed in Table 3 and plotted in Fig. 6. $\delta^{13}C$ values from the fluvial deposit range from −9.92‰ to -8.63‰ and exhibit a mean value of −9.21 ± 0.37‰ (1σ, *n* = 21). Oxygen isotope values from the fluvial deposits range from −7.66‰ to −6.82‰ and exhibit a mean value of −7.24 ± 0.24‰ (1σ, *n* = 21). The $\delta^{13}C$ of the perched deposits range from −9.24‰ to −6.61‰ with a mean value of −7.92 ± 0.74‰ (1σ, *n* = 19) and the corresponding $\delta^{18}O$ values range from −7.85‰ to −6.77‰ with a mean of −7.21 ± 0.35‰ (1σ, *n* = 19).

6. Discussion

5.1 Comparison of perched and fluvial deposits

On the basis of field observations and geomorphology, the (1) substantially thicker, (2) highly eroded, and (3) elevated nature of the perched deposits suggests they formed during an earlier depositional regime, when the water table was markedly higher (~10 m higher) than it is today. Facies contrasts between modern and ancient deposits have been reported in the literature from other arid and semi-arid environments. In these cases, although spring flow is often active under modern conditions, locations around the spring vent contain carbonate remnants situated at elevated positions above active springs indicating a drop in the local water table (e.g., Martin-Algarra et al., 2003; Crombie et al., 1997; Dominguez-Villar et al., 2011; Filho et al., 2012). The similarity in morphology of our system compared with those reported elsewhere, suggests a significant hydroclimate change from higher rainfall (perched deposits) to the present semi-arid conditions (fluvial deposits).

In addition to geomorphic differences, the textures of the fluvial and perched deposits are distinct at the meso- and micro-scale (compare Figs. 3E-F with Figs. 4E-F). The banded morphology of the fluvial deposits is a primary depositional feature typical of freshwater carbonates (e.g., Kano et al., 2004; Andrews and Brasier, 2005; Golubić et al., 2008). The bands reflect calcite deposition associated with microalgae that alternates with pyramidal sparidic bands (Ibarra et al., 2014). In some cases sub-mm diameter pores reflect molds of decayed organic material that represent the former presence of the microalgae *Oocardium stratum* (Ibarra et al., 2014). The continuous nature of the micritic and sparry bands along with well-preserved microalgal calcite molds strongly suggests the pore space between the bands is largely primary (Fig. 3F).

In contrast to the fluvial deposit, the highly indurated texture and vuggy porosity of the perched carbonates suggests they have experienced significant meteoric dissolution and cementation. Vuggy porosity (Fig. 4E) is considered secondary porosity usually resulting from the dissolution of calcareous cements (Tucker and Wright, 1990). The patchy distribution and dominantly micritic nature of the microfabric are typical features of cements that form in the vadose zone, the zone of undersaturation above the water table (Tucker and Wright, 1990). The lack of clear stratigraphic structure at the mesoscale (Fig. 4E) together with microscopic textures that vary at the micrometer scale (Fig. 4F) indicate the perched deposits have undergone several episodes of dissolution and precipitation.

Textural comparisons between the perched and fluvial deposits reveal different diagenetic histories despite proximity. Although diagenesis in tufa deposits is not necessarily only dependent on the age of the deposits (Pentecost, 1981), the striking contrast between the samples that originate from the perched deposit compared to carbonate samples collected along the fluvial channel together with geomorphic differences strongly suggests the perched carbonates are older. Furthermore, differences in carbonate $\delta^{13}C$ between the perched and fluvial deposits may be diagenetic where relatively higher $\delta^{13}C$ values of the perched carbonates compared to the fluvial carbonates may have resulted from progressive dissolution and precipitation caused by percolating rainwater (Janssen et al., 1999). The lack of a clear difference in $\delta^{18}O$ between the two deposits (Fig. 6) may be due to diagenetic alteration caused by spring water values with a similar $\delta^{18}O$ value to the water that originally deposited the carbonate (e.g., Andrews and Brasier, 2005).

Considered together, the (1) geomorphic, (2) textural, and (3) geochemical observations described above together with ^{14}C and IRSL ages constitute compelling evidence that the fluvial and perched deposits reflect distinct depositional periods. The perched deposits formed when the water table was substantially higher (by at least 10 m), producing thick cascade deposits that have since undergone significant erosion (Fig. 4D). In our palaeoenvironmental interpretation below, we focus on the ages obtained for the perched cascade, as carbonate formation about 10 m above modern spring outflow is directly indicative of past pluvials. Our dating of the perched cascade suggests at least two episodes of carbonate growth, one ranging from about 19.4 ± 2.4 to 17.8 ± 2.8 ka and the other at 11.9 ± 1.5 ka (Fig. 7A; Table 1). These pluvials were much wetter than anything in recent history having formed when the water table was ~10 m higher and likely persisting over thousands of years.

5.2.1 Comparison to regional evidence for wet conditions ca. 19 ka

Although there is extensive evidence for substantially wetter conditions across the western US, few of the records available represent coastal settings close to the modern metropolitan centers. Our dated tufa deposits provide ages of carbonate growth representing substantially wetter conditions than present at this coastal site. Based on stratigraphic relationships at the outcrop scale, it is likely that earlier pluvials also existed although the timing of earlier tufa deposition remains to be determined. We focus on comparisons from relatively proximal coastal sites given recent investigations that highlight key spatiotemporal differences in hydroclimate between inland and coastal sites (Lyle et al., 2012; Kirby et al., 2013). *Pinus* pollen in the marine sediments of Ocean Drilling Program (ODP) Site 893 in the Santa Barbara Basin (SBB) about 50 km south of our study site record several episodes of *Pinus* expansion (Fig. 7B) interpreted as wet and/or cold conditions (Heusser and Sirocko, 1997). *Pinus* pollen is well transported by wind and likely sourced from trees in a near coast region (Heusser, 2000), including from the *Pinus* vegetation in the Zaca Lake catchment, which is native although today enhanced by Forest Service planting and fire suppression (Norris and Norris, 1994). The onset of a long-lasting wet event at around 21 ka (Lyle et al., 2012) from the *Pinus* record correlates well with our age estimates of carbonate deposition for the two inner parts of the perched core (Fig. 7A). Additionally, a record of grain size (Kirby et al., 2013; Fig. 7C) and leaf wax δD from Lake Elsinore located about 275 km southeast of our site provide corroborating evidence for a wet late glacial overlapping with the timing of tufa deposition at our site. Tufa deposition strengthens the evidence for pulses of wet conditions during the late glacial in coastal southern California with at least two intervals (ca. 19 and 12 ka) when sustained wet conditions supported a water table approximately 10 m higher than modern and substantial carbonate precipitation.

5.2.2 Comparison to regional evidence for wet conditions ca. 12 ka

The Younger Dryas (YD) is a well-known cold period that interrupted the warming out of the last glacial in the North Atlantic region (Berger, 1990). Although the cooling effects of the Younger Dryas may not have been global, glaciers were reported to have advanced in the Sierra

Nevada Mountains approximately coinciding with the YD whether due to cooling or wetter conditions or both (Phillips et al., 2009), and SSTs in the SBB cooled as the California Current strengthened (Fig. 7D; Pak et al., 2012). In the interior western US, the YD coincided with a wet period with abrupt onset and termination (Wagner et al., 2010; Asmerom et al., 2012). In coastal western US the changes in precipitation during the YD (Fig. 7E) are less clear as a result of dating uncertainties in a variety of records as reviewed by Kirby et al. (2013). Grain size and $\delta D_{(wax)}$ data from well-dated, high-resolution records from Lake Elsinore suggest no substantial increase in precipitation during the YD (Fig. 7C). Rather, the onset of the YD at Lake Elsinore is characterized by an abrupt onset towards less run-off and no obvious change in storm moisture source (Kirby et al., 2013). Furthermore, there is no apparent termination to the YD; rather, conditions continue to remain dry into the Holocene (Kirby et al., 2013). In contrast, the ages of the tufa deposits in the Zaca Lake catchment from our study indicate wet conditions during the YD. Two age constraints –based on independent techniques– date inclusions within the perched tufa and indicate tufa growth: a radiocarbon date on charcoal (10.95 ± 0.12 cal ka BP) and an IRSL age estimate (11.9 ± 1.5 ka) on silicate grains (Fig. 7A). Together, these ages provide compelling evidence for carbonate growth at ca. 12 ka. Carbonate growth of the perched tufa, 10 m higher than the present water table, is necessarily associated with conditions that are wetter than present.

Local cooling is possible because of a decrease in SSTs in the SBB (Fig., 7D; Pak et al., 2012). The *Pinus* pollen record from the SBB also yields evidence for wetter terrestrial conditions (Fig. 7B; Heusser and Sirocko, 1997; Lyle et al., 2012). Our dated tufa deposit matches the last extreme wet event in the *Pinus* record (Fig. 7B). Although at much lower temporal resolution, our record corroborates the SBB record of terrestrial environments, demonstrating the presence of a wet interval that supported carbonate precipitation at the Zaca tufa site and *Pinus* expansion across the area of Santa Barbara County that supplies pollen to the SBB. Another explanation for wetter winters during the YD at Zaca Lake may be related to a shift in average winter season storm tracks. A small shift north in the average position of the winter season storm track could explain wet winters at Zaca as recorded by the tufa growth and mesic pollen in the SBB while at the same time generating dry winters with no apparent change in moisture source at Lake Elsinore, 275 km southeast of Zaca. If true, these data indicate that rather small latitudinal shifts in the average winter season storm track can produce large changes in regional hydroclimates.

Two other peak wet events are recorded from pollen records in marine sites offshore Santa Cruz, CA (ODP site 1018) and at the California-Oregon border (ODP site 1019; Lyle et al., 2012). At ODP site 1018 a significant decline in the prevalence of herbs and shrubs is interpreted as the initiation of a prominent wet event in the area at ca. 11 ka (Lyle et al., 2012). This data matches well with an extended wet interval observed from Moaning Cave on the western foothills of the Sierra Nevada that lasted from about 12.4 ka to about 9.6 ka (Oster et al., 2009). Further, the occurrence of a peak wet event off the coast near the California-Oregon border at ODP site 1019 based on *Alnus* (alder) pollen also coincides with our tufa record (Lyle et al., 2010; 2012). Thus far, comparisons between pollen records in northern and southern California suggest southern California experienced a peak wet event about 6 ka earlier than central and northern coastal California (Lyle et al., 2010; Lyle et al., 2012). Our new tufa record, however, suggests coastal southern California remained substantially wet at ca. 12 ka thus potentially coinciding with wet events north of our site, and challenging the time-transient wet event proposed.

5.2.3 Missing wet events not captured in the tufa record

Although tufa growth at the perched cascade coincides with the last wet event recorded in the SBB *Pinus* record, there are numerous earlier *Pinus* events that we have not resolved in the Zaca tufa record to date. Many of these *Pinus* events are captured in the Elsinore sand record as intervals of enhanced run-off. *Pinus* reached a maximum between 14−17 ka, with additional brief wet events at about 14.1 and 13.3 ka. In particular, the peak in *Pinus* event at ca. 16 ka is not particularly well-represented in the tufa, though we note it is within the age uncertainty. The surficial nature of tufa deposition inherently introduces potential for episodes of erosion and/or non-deposition (Andrews and Brasier, 2005) possibly resulting from spring water flow diversion to other channels around the vent. At the moment however, with the current age uncertainty and dating resolution available on the tufa, it is difficult to fully resolve the timing of tufa growth during the wettest interval recorded by offshore marine sediments (Lyle et al., 2010). It is encouraging, however, that both of our main wet events as recorded by the tufa (ca. 19 ka and ca. 12 ka) entirely span the observed long-lived wet event derived from marine records 50 km away (Lyle et al., 2012). Our record thus provides an important complementary addition to evidence for past pluvials in coastal southern California.

6. Conclusions

We present ^{14}C and IRSL dates of perched and fluvial tufa deposits from a coastal site in Santa Barbara county, California revealing at least two late glacial pluvials. Geomorphic, textural, petrographic, and geochemical distinctions between perched and fluvial deposits reflect a transition from a wetter climate regime that resulted in the formation of the perched deposits to the present actively-accreting fluvial carbonates (located about 10 m below the perched deposits) along the modern spring flow path. Luminescence dates indicate the perched tufa cascade was active from about 19.4 ± 2.4 to about 17.8 ± 2.8 ka. These ages agree with independent records that also suggest wetter coastal conditions at these times. A second wet event dated to 11.9 ± 1.5 ka based on luminescence and verified with a dated charcoal inclusion to 10.95 ± 0.12 ka BP indicate the Late Pleistocene early Holocene transition was also wetter than present. Ages for the perched deposits provide a new record of past pluvial conditions for the region, highlighting the utility of fluvial tufa as a terrestrial record of water balance.

7. Acknowledgements

We thank the Zaca Lake Retreat Staff for access to Zaca Lake. We thank K. Zacny, G. Paulson, L. Beegle, A. Lopez, M. Cheetham, and A. Bardsley for field assistance, M. Rincon for isotopic analyses of carbonates and W. Barrera for assistance with luminescence analyses. We also thank W. Berelson and S. Lund for helpful discussions. This research was supported by the Geological Society of America graduate student research grant to Y.I., US National Science Foundation Grant EAR-1002656 to S.F. and M.K. and a US National Aeronautics and Space Administration SBIR Phase II grant to Honeybee Robotics Ltd and the University of Southern California.

8. References

Adamiec, G., Aitken, M.J., 1998. Dose-rate conversion factors: new data. Ancient TL 16, 37-50.

Andrews, J.E., 2006. Palaeoclimatic records from stable isotopes in riverine tufas: Synthesis and review. Earth Science Reviews 75, 85-104.

Allen, B.D., and Anderson, R.Y., 2000, A continuous, high-resolution record of late Pleistocene climate variability from the Estancia basin, New Mexico: Geological Society of America Bulletin, v. 112, p. 1444-1458.

Anderson, R.Y., Allen, B.D., and Menking, K.M., 2002, Geomorphic expression of abrupt climate change in Southwestern North America at the glacial termination: Quaternary Research, v. 57, p. 371-381.

Andrews, J.E., Brasier, A.T., 2005. Seasonal records of climatic change in annually laminated tufas: short review and future prospects. Journal of Quaternary Science 20, 411-421.

Asmerom, Y., Polyak, V.J., Burns, S.J., 2010. Variable winter moisture in the southwestern United States linked to rapid climate shifts. Nature Geoscience 3, 114-117.

Auler, A.S., Smart, P.L., 2001. Late Quaternary Paleoclimate in Semiarid Northeastern Brazil from U-Series Dating of Travertine and Water-Table Speleothems. Quaternary Research 55, 159-167.

Barnes, I., 1965. Geochemistry of Birch Creek, Inyo County, California a travertine depositing creek in an arid climate. Geochimica et Cosmochimica Acta 29, 85-112.

Benson, L.V., Currey, D.R., Dorn, R.I., Lajoie, K.R., Oviatt, C.G., Robinson, S.W., Smith, G.I., Stine, S., 1990. Chronology of expansion and contraction of four Great Basin lake systems during the past 35,000 years. Palaeogeography, Palaeoclimatology, Palaeoecology 78, 241-286.

Berger, W. H., 1990. The younger dryas cold spell—a quest for causes. Global and Panetary Change 3, 219-237.

Briggs, R.W., Wesnousky, S.G., Adams, K.D., 2005. Late Pleistocene and late Holocene lake highstands in the Pyramid Lake subbasin of Lake Lahontan, Nevada, USA. Quaternary Research 64, 257-263.

Buylaert, J.P., Murray, A.S., Thomsen, K.J., Jain, M., 2009. Testing the potential of an elevated temperature IRSL signal from K-feldspar. Radiation Measurements 44, 560-565.

Cayan, D.R., Roads, J.O., 1984. Local Relationships between United States West Coast Precipitation and Monthly Mean Circulation Parameters. Monthly Weather Review 112, 1276-1282.

Cook, E.R., Woodhouse, C.A., Eakin, C.M., Meko, D.M., Stahle, D.W., 2004. Long-term aridity changes in the western United States. Science 306, 1015-1018.

Cremaschi, M., Zerboni, A., Spo˜ tl, C., Felletti, F., 2010. The calcareous tufa in the Tadrart Acacus Mt. (SW Fezzan, Libya) An early Holocene palaeoclimate archive in the central Sahara. Palaeogeography, Palaeoclimatology, Palaeoecology 287, 81-94.

Crombie, M.K., Arvidson, R.E., Sturchio, N.C., Alfy, Z.E., Zeid, K.A., 1997. Age and isotopic constraints on Pleistocene pluvial episodes in the Western Desert, Egypt. Palaeogeography, Palaeoclimatology, Palaeoecology 130, 337-355.

Denton, G.H., Anderson, R.F., Toggweiler, J.R., Edwards, R.L., Schaefer, J.M., and Putnam, A.E., 2010, The last glacial termination: Science, v. 328, p. 1652-1656.

Domínguez-Villar, D., Vázquez-Navarro, J.A., Cheng, H., Edwards, R.L., 2011. Freshwater tufa record from Spain supports evidence for the past interglacial being wetter than the Holocene in the Mediterranean region. Global and Planetary Change 77, 129-141.

Feakins, S.J., Kirby, M.E., Cheetham, M.I., Ibarra, Y., and Zimmerman, S.R.H., 2014, Fluctuation in leaf wax D/H ratio from a southern California lake records significant variability in isotopes in precipitation during the late Holocene: Organic Geochemistry, v. 66, p. 48-59.

Filho, W.S., Almeida, L.H.S., Boggiani, P.C., Karmann, I., 2012. Characterization of quaternary tufas in the Serra do Andre Lopes karst, southeastern Brazil. Carbonates and Evaporites 27, 357-373.

Garnett, E.R., Andrews, J.E., Preece, R.C., Dennis, P.F., 2004. Climatic change recorded by stable isotopes and trace elements in a British Holocene tufa. Journal of Quaternary Science 19, 251-262.

Golubić, S., Violante, C., Plenković-Moraj, A., Grgasović, T.i., 2008. Travertines and calcareous tufa deposits: an insight into diagenesis. Geologia Croatica 61, 363-378.

Heusser, L.E., Sirocko, F., 1997. Millennial pulsing of environmental change in southern California from the past 24 k.y.: A record of Indo-Pacific ENSO events? Geology 25, 243-246.

Ibarra, Y., Corsetti, F.A., Cheetham, M.I., Feakins, S.J., 2014. Were fossil spring-associted carbonates near Zaca Lake, Santa Barbara, California deposited under an ambient or thermal regime? Sedimentary Geology 301, 15-25.

Janssen, A., Swennen, R., Podoor, N., Keppens, E., 1999. Biological and diagenetic influence in Recent and fossil tufa deposits from Belgium. Sedimentary Geology 126, 75-95.

Kano, A., Kawai, T., Matsuoka, J., and Ihara, T., 2004, High-resolution records of rainfall events from clay bands in tufa: Geology, v. 32, p. 793-796.

Kirby, M.E., Feakins, S.J., Bonuso, N., Fantozzi, J.M., Hiner, C.A., 2013. Latest Pleistocene to Holocene hydroclimates from Lake Elsinore, California. Quaternary Science Reviews 76, 1-15.

Kirby, M.E., Lund, S.P., Poulsen, C.J., 2005. Hydrologic variability and the onset of modern El Niño –Southern Oscillation: a 19 250-year record from Lake Elsinore, southern California. Journal of Quaternary Science 20, 239-254.

Lyle, M., Heusser, L., Ravelo, C., Yamamoto, M., Barron, J., Diffenbaugh, N.S., Herbert, T., Andreasen, D., 2012. Out of the Tropics: The Pacific, Great Basin Lakes, and Late Pleistocene Water Cycle in the Western United States. Science 337, 1629-1633.

Lyle, M., Heusser, L., Ravelo, C., Andreasen, D., Lyle, A.O., and Diffenbaugh, N., 2010, Pleistocene water cycle and eastern boundary current processes along the California continental margin: Paleoceanography, v. 25, p. PA4211,

Mensing, S.A., 2001. Late-Glacial and Early Holocene Vegetation and Climate Change near Owens Lake, Eastern California. Quaternary Research 55, 57-65.

Mensing, S.A., Sharpe, S.E., Tunno, I., Sada, D.W., Thomas, J.M., Starratt, S., Smith, J., 2013. The Late Holocene Dry Period: multiproxy evidence for an extended drought between 2800 and 1850 cal yr BP across the central Great Basin, USA. Quaternary Science Reviews 78, 266-282.

Newton, M.S., Grossman, E.L., 1988. Late Quaternary chronology of tufa deposits, Walker Lake, Nevada. Journal of Geology 96, 417-433.

Norris, J., Norris, L., 1994. History of Zaca Lake. Olive Press Publications, Los Olivos.

Oster, J.L., Montañez, I.P., Sharp, W.D., and Cooper, K.M., 2009, Late Pleistocene California droughts during deglaciation and Arctic warming: Earth and Planetary Science Letters, v. 288, p. 434-443

Pak, D.K., Lea, D.W., and Kennett, J.P., 2012, Millennial scale changes in sea surface temperature and ocean circulation in the northeast Pacific, 10–60 kyr BP: Paleoceanography, v. 27, p. PA1212,doi:10.1029/ 2011PA002238.

Pedley, H.M., 1990. Classification and environmental models of cool freshwater tufas. Sedimentary Geology 68, 143-154.

Pentecost, A., 1981. The Tufa Deposits of the Malham District, North Yorkshire. Field Studies 5, 365-387.

Pentecost, A., Zhang, Z.-H., 2008. Microfossils and geochemistry of some modern, Holocene and Pleistocene travertines from North Yorkshire and Derbyshire. Proceedings of the Yorkshire Geological Society 57, 79-94.

Phillips, F.M., Zreda, M., Plummer, M.A., Elmore, D., and Clark, D.H., 2009, Glacial geology and chronology of Bishop Creek and vicinity, eastern Sierra Nevada, California: Geological Society of America Bulletin, v. 121, p. 1013-1033.

Rhodes, E.J., Dating sediments using potassium feldspar single-grain IRSL: initial methodological considerations. Quaternary International, submitted Jan 2014.

Scholl, D.W., 1960. Pleistocene algal pinnacles at Searles Lake, California. Journal of Sedimentary Petrology 30, 414-431.

Seager, R., Ting, M., Held, I., Kushnir, Y., Lu, J., Vecchi, G., Huang, H.-P., Harnik, N., Leetmaa, A., Lau, N.-C., Li, C., Velez, J., Naik, N., 2007. Model Projections of an Imminent Transition to a More Arid Climate in Southwestern North America. Science 316, 1181-1184.

Szabo, B.J., 1990. Ages of Travertine Deposits in Eastern Grand Canyon National Park, Arizona. Quaternary Research 34, 24-32.

Tucker, M.E., and Wright, V.P., 1990, Carbonate Sedimentology, Blackwell Scientific Publications.

Viles, H.A., Taylor, M.P., Nicoll, K., Neumann, S., 2007, Facies evidence of hydroloclimatic regime shifts in tufa depositional sequences from the arid Naukluft Mountains, Namibia. Sedimentary Geology 195, 39-53.

Wagner, J.D.M., Cole, J.E., Beck, J.W., Patchett, P.J., Henderson, G.M., Barnett, H.R., 2010. Moisture variability in the southwestern United States linked to abrupt glacial climate change. Nature Geoscience 3, 110-113.

Wells, S.G., Brown, J.B., Enzel, Y., Anderson, R.Y., and McFadden, L.D., 2003, Late Quaternary geology and paleohydrology of pluvial Lake Mojave, southern California, *in* Enzel, Y., Wells, S.G., and Lancaster, N., eds., Paleoenvironments and Paleohydrology of the Mojave and Southern Great Basin Deserts: Boulder, CO, Geological Society of America, p. 79-115.

Figure Captions

Fig. 1. Study site. (A) Geologic map of the study area. Abbreviations: M = Monterey; Qs = surface Quaternary; L = landslide; Tv = Tertiary volcanics. Dashed lines denote fault lines. Contours are at 200 m intervals. (B) Regional map denoting locations mentioned in the text.

Fig. 2. Schematic of carbonate facies modified from Viles et al., 2007 (figure not drawn to scale; the approximate distance from the boxed spring to the fluvial cascade is 180 m).

Fig. 3. Multiscale facies of the fluvial carbonates. (A) Terminal fluvial cascade with people on the outcrop for scale. (B) Distinct carbonate growth episodes along the fluvial cascade with a basal white carbonate layer (1) and draping brown carbonate layer (2). (C) Carbonate-encrusted organic debris and plant molds along the fluvial terminal cascade. (D) Carbonate-encrusted twig located near the fluvial channel. (E) Banded carbonate from the fluvial cascade. (F) Photomicrograph of (E), blue areas denote pore space.

Fig. 4. Multiscale facies of the perched carbonates. (A) Dipping carbonate block showing location of the 'dark core'. (B) Carbonate curtains of the cascade face, bottom. (C) Carbonate curtains of the cascade face, top. (D) Carbonate talus blocks along the valley slope, looking

northeast. (E) Mesostructure of the perched carbonates with distinct vuggy pores. (F) Photomicrograph of (E), blue areas denote pore space.

Fig. 5. (A) Location of 'dark core' collected for OSL. (B) Carbonate-encrusted root for which carbonate (sample ZC-F-root) and organic carbon (sample ZC-F-carb) ^{14}C was measured.

Fig. 6. Cross plot of carbonate carbon and oxygen stable isotope values of the fluvial and perched deposits.

Fig. 7. Regional comparisons. (A) IRSL measurements from this study and ^{14}C of charcoal. (B) *Pinus* pollen record from ODP site 893 in the Santa Barbara Basin (Heusser and Sirocko, 1997). (C) Record of percent sand from Lake Elsinore (Kirby et al., 2013). (D) Ca/Mg record from ODP site 1017E near the Santa Barbara Basin (Pak et al., 2012). (E) NGRIP $\delta^{18}O$ record from Greenland highlighting the Last Glacial Maximum (LGM), Older Dryas (OD), Bolling-Allerod (BA), and Younger Dryas (YD) intervals (North Greenland Ice Core Project members, 2004).

Figure 1

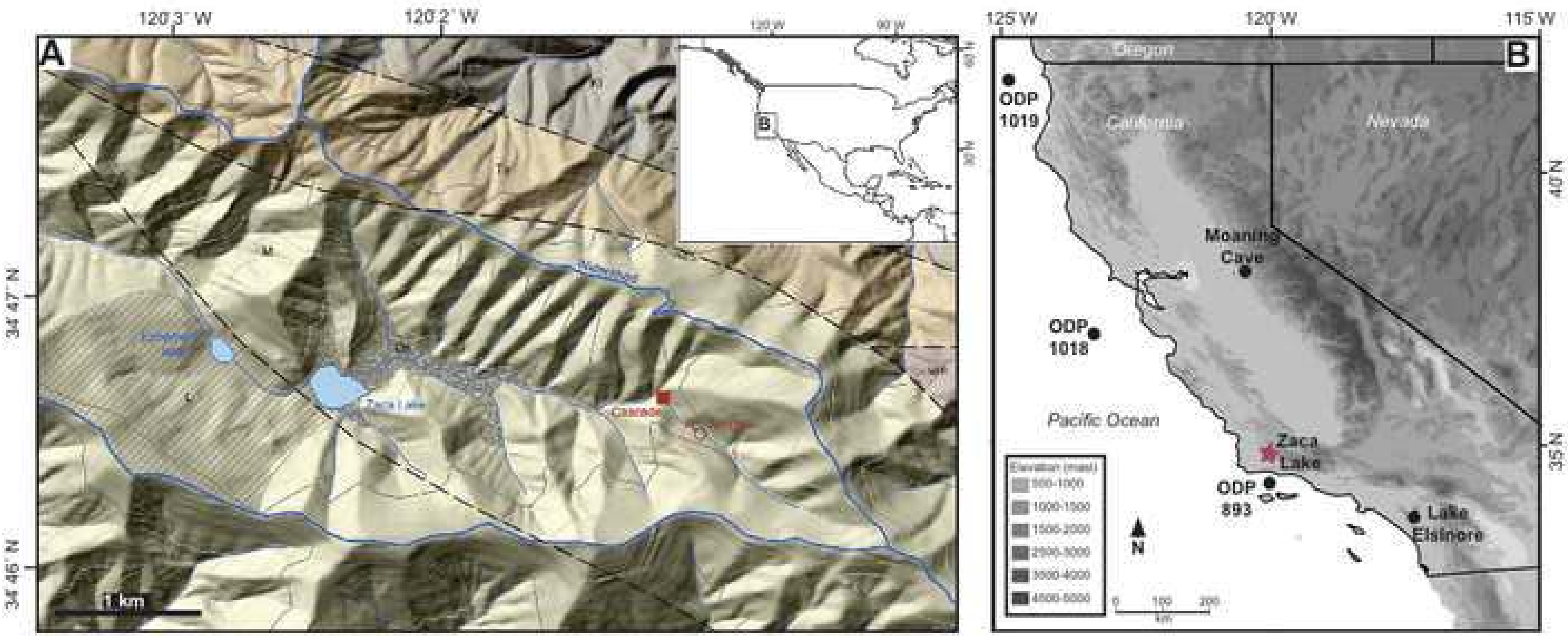
120°3' W
120°2' W
34°47' N
34°46' N
A
1 km
Zaca Lake
B
125°W
120°W
115°W
40°N
35°N
Oregon
California
Nevada
ODP 1019
ODP 1018
Moaning Cave
Pacific Ocean
Zaca Lake
ODP 893
Lake Elsinore
N
0 100 200

Figure 2
Click here to download high resolution image

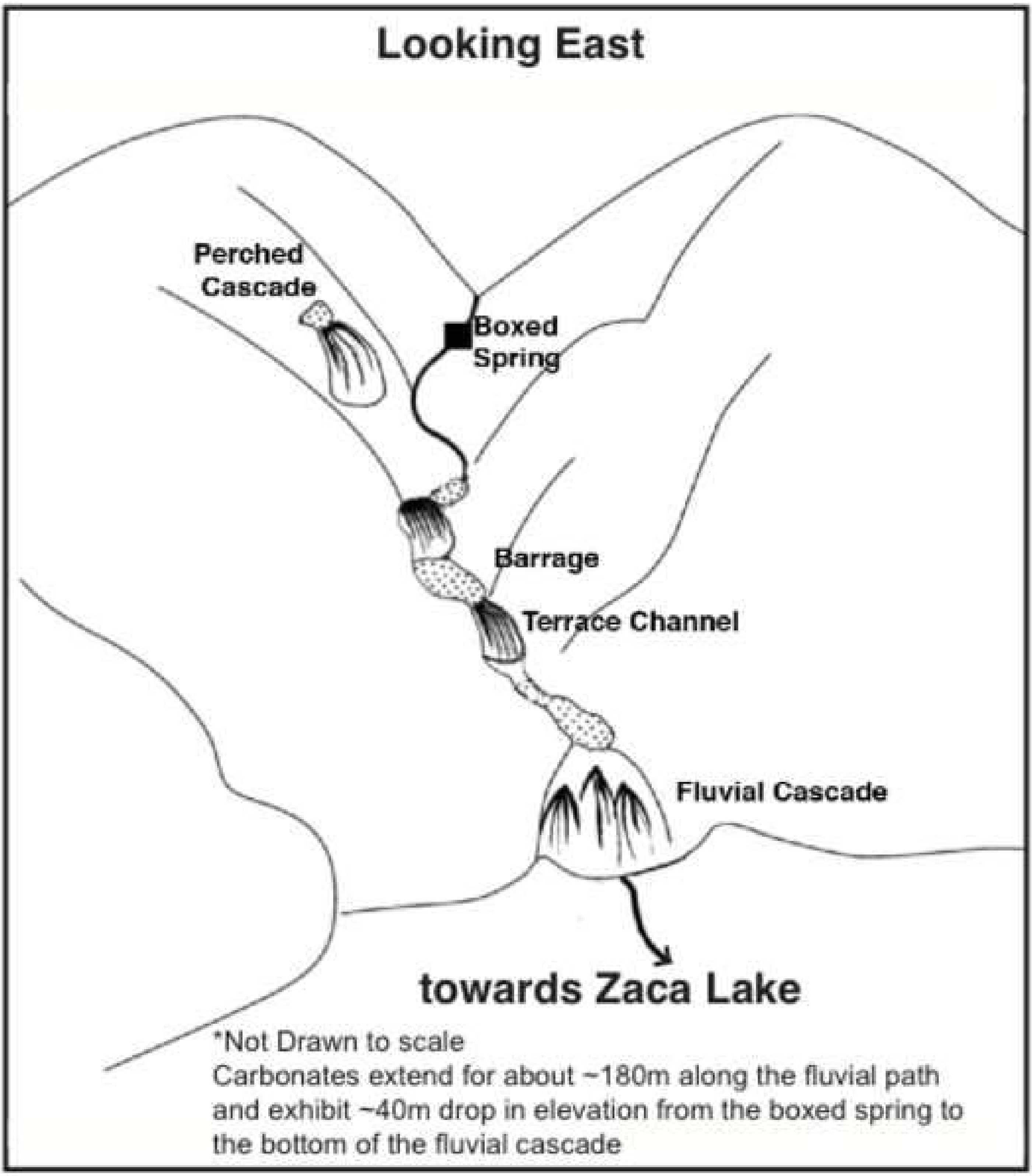

Figure 3
Click here to download high resolution image

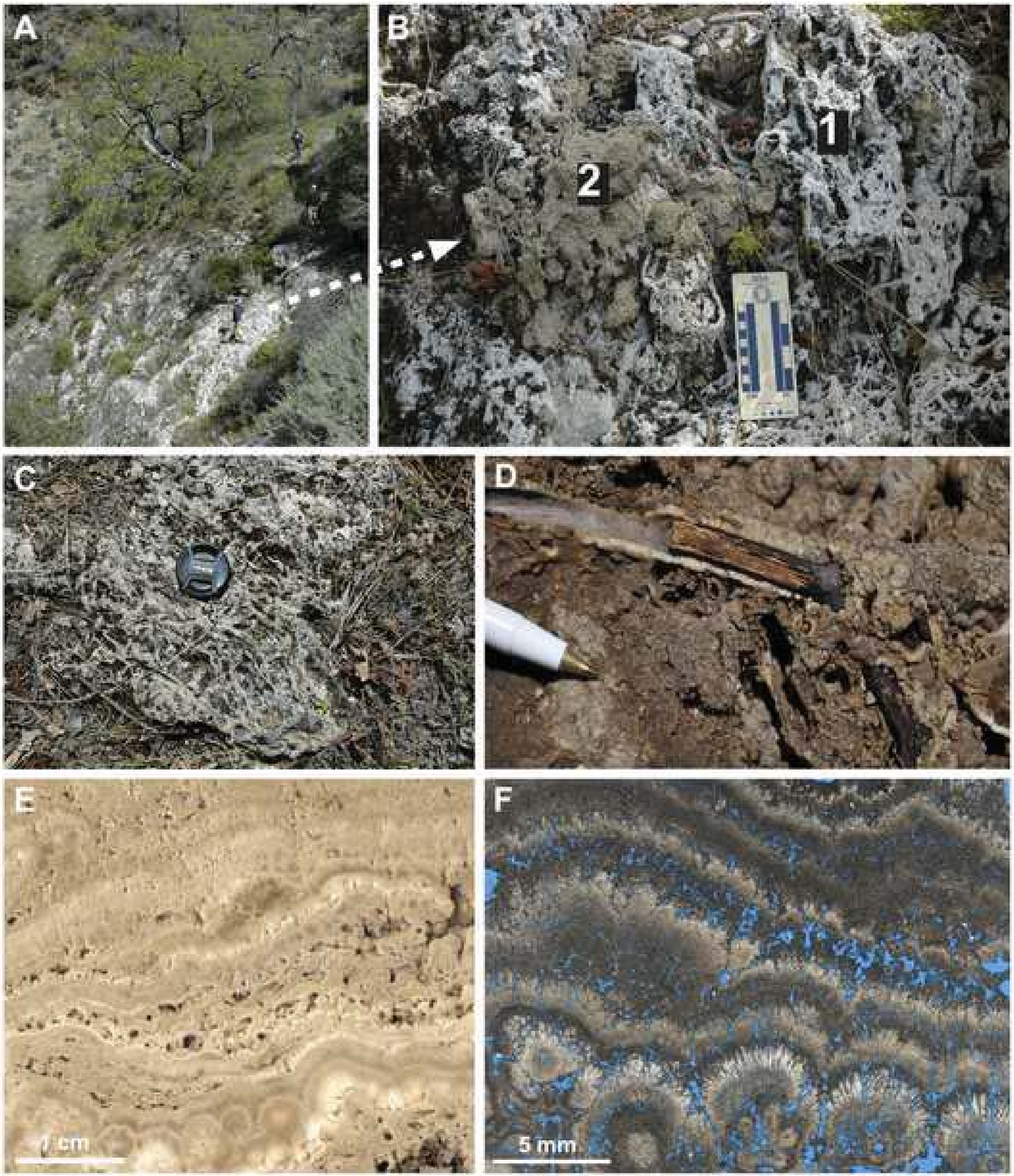

Figure 4
Click here to download high resolution image

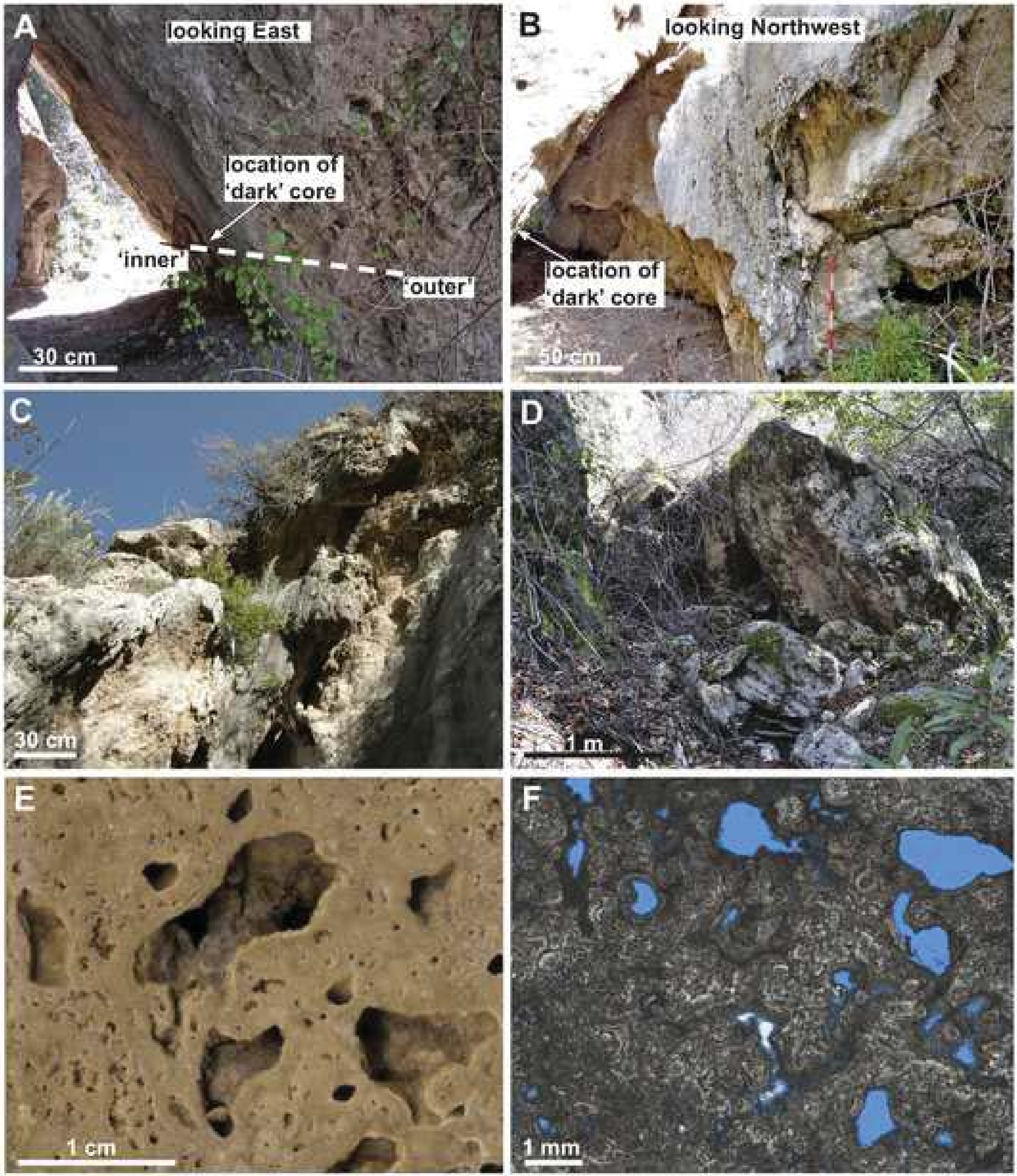

Figure 5
Click here to download high resolution image

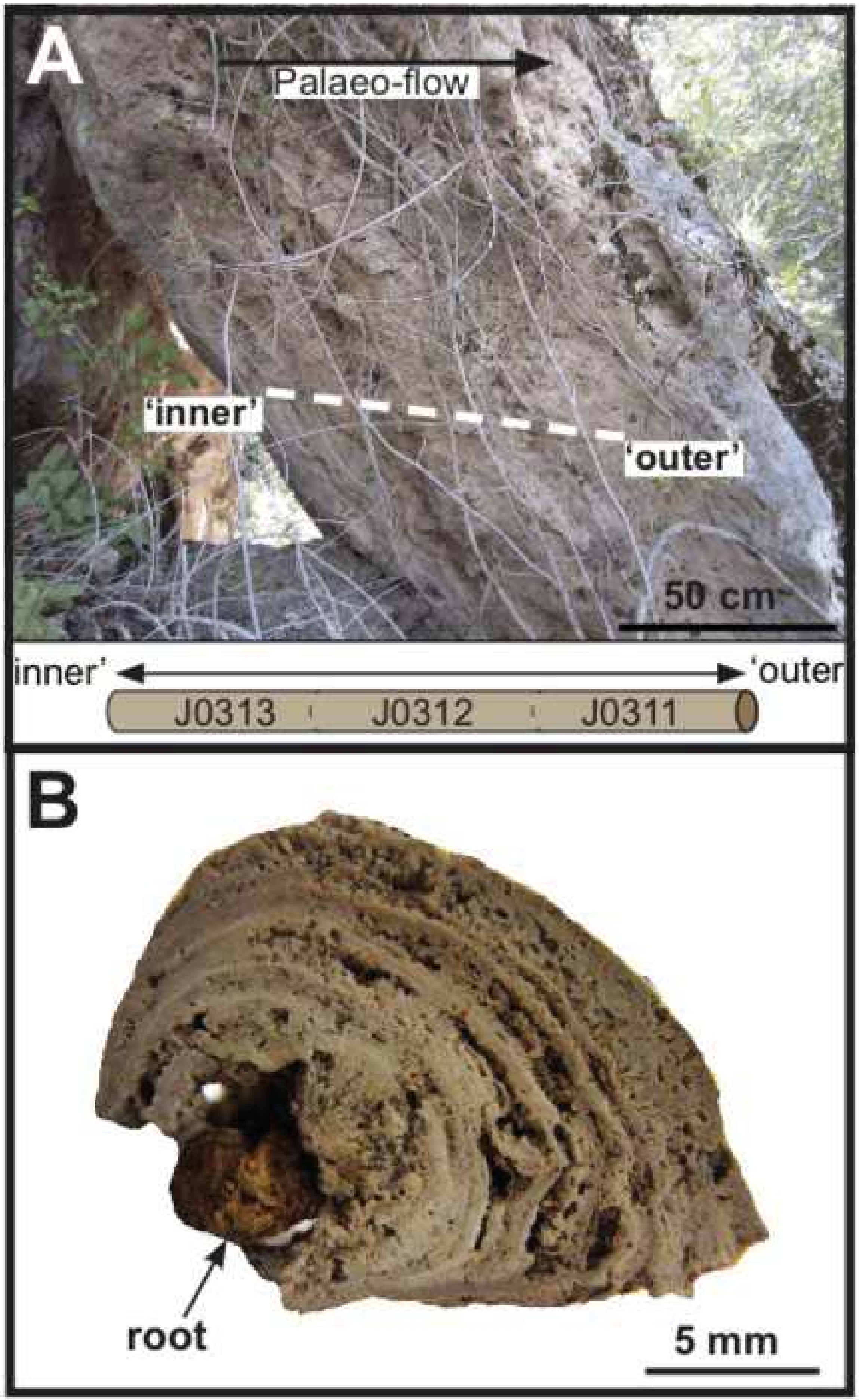

Figure 6

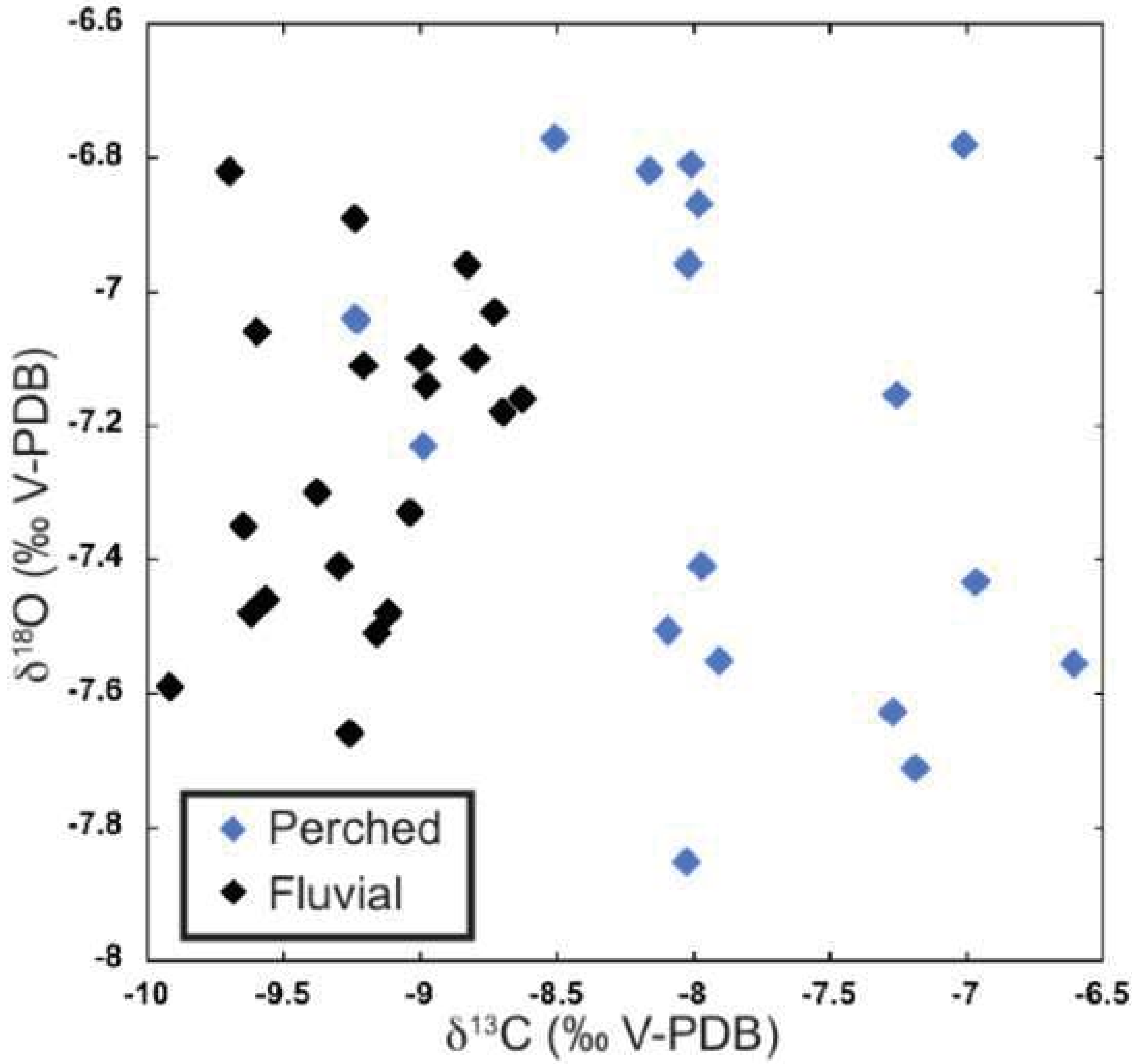
-6.6
-6.8
-7
-7.2
-7.4
-7.6
-7.8
-8
δ18O (‰ V-PDB)
-10
-9.5
-9
-8.5
-8
-7.5
-7
-6.5
δ13C (‰ V-PDB)
Perched
Fluvial

Figure 7

Click here to download high resolution image

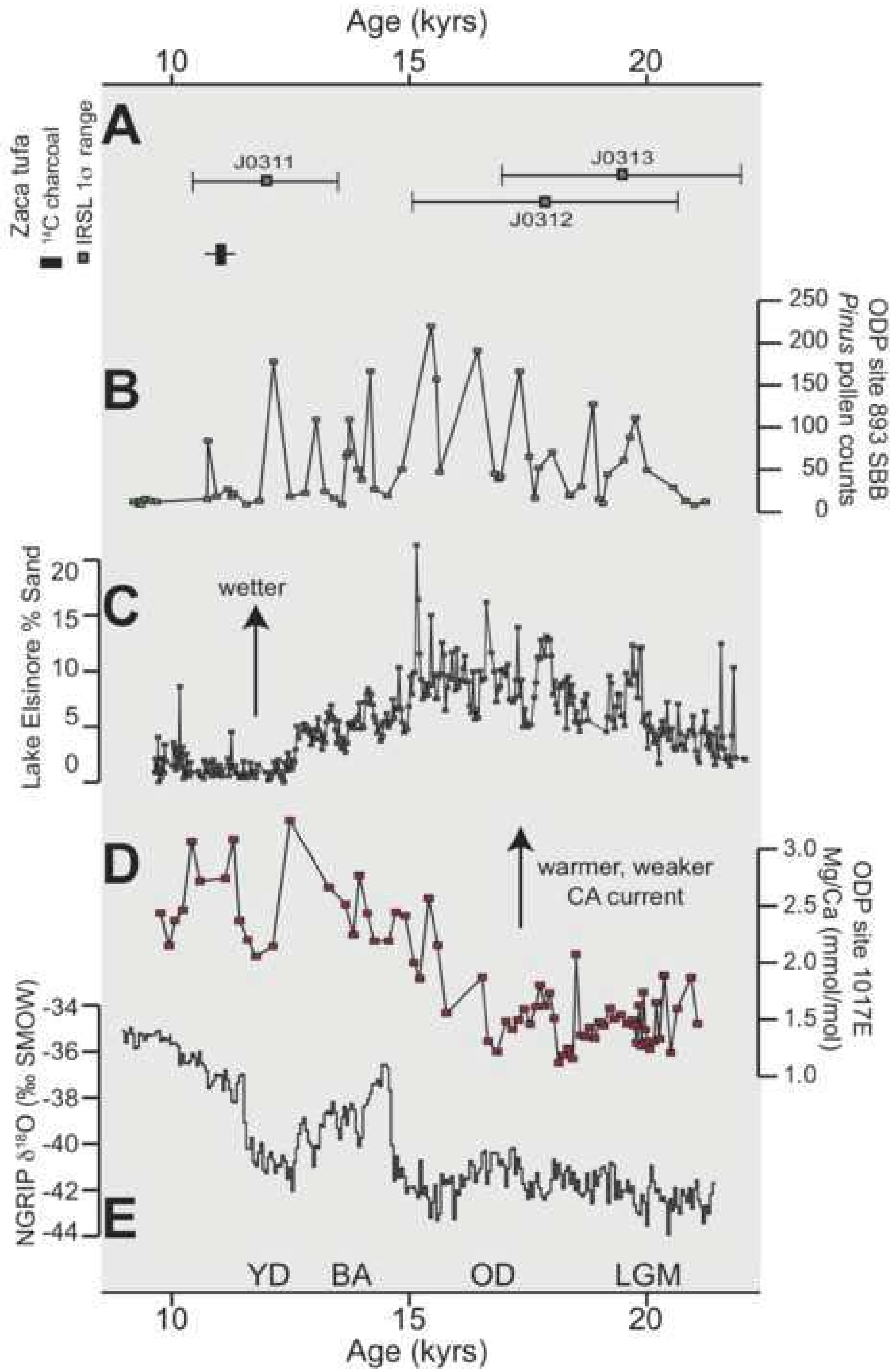

Table 1 IRSL measurement values of carbonate samples from the perched cascade core.

Lab Code	D_e (Gy) ± 1 σ	Dose rate (mGy/a) ± 1 σ	Age (years before AD 2014)
J0311	11.8 ± 1.2	0.99 ± 0.07	11,900 ± 1,500
J0312	18.3 ± 2.5	1.02 ± 0.07	18,000 ± 2,800
J0313	20.3 ± 2.1	1.05 ± 0.07	19,400 ± 2,400

Table 2
Click here to download Table: UCIAMS3.doc

Ā Ā
Ā

Table 2 %(0Ā=CĀ@=MKĀK>IHMĀ=H@CĀHE?LĀKQ=?MA@ĀBKIGNOMAH@BAJDK@Ā@AJILEML

:0 3. 59ĀĀ9=GJFA3ĀĀ	%(0 Ā=CĀĀ Ā/7 Ā	SĀ	&σĀ8=HCĀ	.CAĀĀ?RĀ 7 =Ā
%%(-*%Ā<0"?=K>Ā	%+!-%$Ā	)$Ā	21,500−21,899Ā	&%!+$$Ā
%&(('-Ā <0"0"?=K>Ā	%)!&%$Ā	($Ā	18,343−18,612Ā	%,!(+,Ā
%&((($Ā <0"2"?=K>Ā	-!%))Ā	&)Ā	10,239−10,304Ā	%$!&+&Ā
%&(((%Ā <0"20"?=K>Ā	-!-*$Ā	&)Ā	11,263−11,410Ā	%%!"+Ā
%&(('$Ā <0"70"?D=KĀ	-!*$$Ā	&)Ā	%$!,'$−%%!$+$Ā	%$!-)'Ā

9=GJFALĀPEMDĀGI@AKHĀ2ĀĀ%(0 Ā	SĀ	; Ā=KĀ.1>Ā	Ā
%%)&*-Ā<0"MPCEĀ	%#%+$'Ā	$#$$&'Ā	%-,+#-Ā
%%)&+$Ā<0"65% Ā	%#%-%-Ā	$#$$&*Ā	%-,,#*Ā
%%)&+%Ā<0"65& Ā	%#$-$-Ā	$#$$&%Ā	%---#-Ā
%&(('%Ā <0"0"MPCEĀ	%#%+,)Ā	$#$$&'Ā	%-,,Ā
%&(('&Ā <0"2"KIIMĀ	%#$*-,Ā	$#$$&%Ā	&$$+Ā

=Ā0=FE>K=MCA@Ā=HĀ43/Ā+#$#%ĀKU7K=GĀĀ9MNOEAKĀAMĀĀ=F#!Ā%--,
>Ā0=FE!G>Ā7KIK=GĀĀ8EGAKMĀĀ=F#!Ā&$%'
Ā
Ā

Table 3

9L<=E@ÂDKHLFHIDKDDHKÂH δ 7Â<G?δ 0ÂÂ‰Â:81 / ÂAIHÂHG<L@ÂIF ÂC@DJÂJ@KIHDGÂ@HKDLÂ

0<J=HGL@Â9<F I E@ÂÂ ?@IHKLÂ		δ 0Â	δ 7ÂÂ
3EMDN<E	; 8HH>%'!Â	"-#*&Â	"+#(, Â
	;= "H>"=Â	"-#&%Â	"+#%&Â
	;= "H>"LÂ	",# , Â	"+#%(Â
	; 8?%'! Â	"-#-&Â	"+#)-Â
	; ="?Â	"-#%&Â	"+#(,Â
	; I?(Â	"-#*$Â	"+#$*Â
	; IHH>%&!Â	",#,$Â	"+#%$Â
	; IHH>()!Â	",#+'Â	"+#$'Â
	; IHH>Â	"-#$$Â	"+#%$Â
	; I?%&Â	"-#+$Â	"*#,&Â
	; I?() !Â	"-#$(Â	"+#"Â
	;7 0&!Â	"-# $Â	"+#(%Â
	70Â	"-#&(Â	"*#,-Â
	30 "$%Â	",#+$Â	"+#%, Â
	30 "$&Â	",#*' Â	"+#%*Â
	30 $' !Â	",#,' Â	"*# *Â
	; . %Â	"-#*) Â	"+#) Â
	;6 %Â	"-#%*Â	"+#) %Â
	; . &Â	"-#) +Â	"+#(*Â
	30 "1 %'%Â	"-#&*Â	"+#**Â
	30 "1 ' !Â	"-#',Â	"+#'$Â
	mean	"-#&%Â	"+#&(Â
	1σ	$#'+Â	$#&(Â
8@>C@Â	;I >"HH>&Â	"+#$%Â	"*#+, Â
Â	;I >"HH>' Â	"+# +Â	"+#(%Â
Â	80 &.Â	",#$&Â	"*#-*Â
Â	; I>"?%Â	",#)%Â	"*#++Â
Â	; I>"?&Â	",#--Â	"+#&'Â
Â	80 &?Â	"-#&(Â	"+#$(Â
Â	80 &.Â	",#$&Â	"*#-*Â
Â	80 &3Â	"+#-,Â	"+#$(Â
Â	80 &4Â	",#$%Â	"*#,%Â
Â	80 &1Â	"-#&(Â	"+#$(Â
Â	80 &2Â	",#%*Â	"*#,&Â
Â	80).Â	"+#&)Â	"+#%)Â
Â	80)/ Â	",#$'Â	"+#,)Â
Â	80)0 Â	"+#-%Â	"+#))Â
Â	80)1Â	",#$-Â	"+#)%Â
Â	80 -.Â	"+#&+Â	"+#*'Â
Â	80 -/ Â	"+#%-Â	"+#+%Â
Â	80 -0 Â	"*#*%Â	"+#)*Â
Â	80 -1Â	"*#-+Â	"+#('Â
Â	**mean**	"+# &Â	"+#&%Â
	1σ	$#+(Â	$#') Â

*9<F I E@ÂÂK@ÂK,ÂJ@K@Â*mean*Â δ 18O and δ 0 ÂHAÂ<LÂE@ÂKÂÂ@LÂ<HBÂC@ÂK@ =<G?